Iranian Journal of Astronomy and Astrophysics
Vol. 12, No. 1, Winter 2025, 99–109
©Available online at http://ijaa.du.ac.ir
DOI: 10.22128/ijaa.2025.2993.1217
Online ISSN: 2383–403X

Iranian Journal of Astronomy and Astrophysics

Research Paper

Observational Insights into Pre-Flare Very Large Pulsations in the Solar Corona

Narges Fathalian*[1] · Malihe Jalalirad[2]

[1] Physics, Basic Sciences, Department, Payame Nour University(PNU), Tehran, Iran;
*email: narges.fathalian@pnu.ac.ir

[2] Physics, Basic Sciences Department, Payame Nour University, Tehran, Iran;
email: arezoo.jalalirad@gmail.com

Received: 16 July 2025; **Accepted:** 8 September 2025; **Published:** 16 September 2025

Abstract. Solar flares are impulsive releases of magnetic energy in the Sun's atmosphere, producing broadband electromagnetic radiation from radio waves through optical and ultraviolet up to X- and gamma-ray photons. Their intensity is quantified by the peak soft X-ray flux in the range of 1 – 8 Å as measured by the GOES satellites, and thus classified—on a logarithmic scale—into A, B, C, M, and X classes, each representing a tenfold increase in flux. Accurate forecasting of both the timing and intensity class of solar flares is essential for mitigating their potentially severe impacts. Among the most promising precursors are very-long-period pulsations (VLPs)—broadband oscillations with reported periods of roughly 8–30 minutes that typically emerge one to two hours before flare onset. In this study, we analyzed GOES 1–8 Å soft X-ray data of three new flares and detected distinctive pre-flare VLP signatures in two M-class events. Measured pulsation periods detected are 25.2 and 20.0 (mixed with a period of 43 minutes), and each event exhibited four to six discrete pulses. Our analysis showed that increasing the number of free parameters in the fitting function can significantly enhance the accuracy of the flux model, as evidenced by improved goodness-of-fit metrics. The remaining third flare in our sample showed no clear VLP activity in the pre-eruption interval.

Keywords: Solar Corona, Solar Flare, Pre-Flare Very Long-period (VLP) Pulsations, Flare Prediction.

1 Introduction

Solar flares are abrupt releases of electromagnetic radiation in the solar atmosphere, typically erupting from magnetically active regions. Their energies span from microflares (10^{26} erg, 10^{19} J) to the most powerful events exceeding (10^{32} erg, 10^{25} J). Magnetic reconnection—driven by complex magnetic-field topologies—rapidly converts stored magnetic energy into kinetic and thermal energy in flares. This process accelerates electrons and ions to relativistic energies, giving rise to hard X-rays (HXRs) and gamma rays, while energetic particle collisions heat the lower atmosphere and produce intense optical, ultraviolet (UV), and soft X-ray emissions. These emissions originate chiefly from compact chromospheric and photospheric sources known as footpoints and ribbons. Additionally, damping of Alfvén waves

* *Corresponding author*

can deliver substantial heat to deep atmospheric layers that particles cannot easily penetrate. Although coronal soft X-ray and UV fluxes peak during flares, they account for only a minor fraction of the total radiative energy measured by broadband radiometers. The intricate coupling of magnetic fields and plasma during flares often generates quasi-periodic pulsations (QPPs)[16]]—quasi-oscillatory signatures defined as repetitive intensity modulations in flare light curves. Such oscillations can be detected in the pre-flare phase as well as the rise and decay phases of flares [7,11].

Solar-flare oscillation periods span from under one second to several hundred seconds, with the exact values determined by the temporal resolution of the observing instrument and the wavelength band being analyzed [8,18,19,23,32]. Despite extensive observational and theoretical efforts, the fundamental mechanism driving QPP production remains incompletely understood [15,29] and is attributed to magnetohydrodynamic waves [27,31] or magnetic reconnection [12,26]. To date, pre-flare phase observations have revealed a host of phenomena—radio spectrum radiations, filament activity, X-ray eruptions, gamma rays, and the like—highlighting the complex signatures that precede flare onset. Analysis of GOES soft X-ray (SXR) data during the pre-flare phase shows that, in some events, very long-period pulsations (VLPs)—oscillatory pulses with extended periodicities—emerge one to two hours before flare onset. Such VLPs, defined by their lengthy time scales, have also been frequently reported in both solar flare and nonflare contexts (see for instance, [6,20,24,30], etc.). Pre-flare VLPs were first introduced and analyzed by Tan et al. (2016) [22]. In their study, they documented four pre-flare VLP events occurring one to two hours prior to the onset of the following flares: an M2.9 flare on 25 October 2013, a C2.4 flare on 13 July 2012, an X2.0 flare on 26 October 2014, and an X2.7 flare on 05 May 2015—as well as C-class flares—with observed periods ranging between 8 and 30 minutes. Subsequently, Li et al. (2020c) reported detecting pre-flare VLPs in the H and EUV211 wavelengths before an M1.1 flare on 16 October 2015, with a measured period of approximately 9.3 minutes. Later, Jalalirad and Fathalian (2022) [9] observed pre-flare VLP pulsations associated with 10 solar flares, exhibiting periods between 14 and 24.9 minutes. Jalalirad and Fathalian (2023) presented the observation of six M- and C-class solar flares that exhibited pre-flare VLPs, with measured periods ranging from 14.6 to 28.2 minutes. [10]. Li et al. (2024) present the first simultaneous detection of very long-period (8.6 min) white-light pulsations in both an X6.4 solar flare and its adjacent sunspot penumbra, using high-cadence observations from space- and ground-based instruments; through Morlet wavelet and Fourier analyses they demonstrate coherent but low-amplitude oscillations that suggest slow-mode magnetoacoustic gravity waves leaking from the penumbra modulate flare emission, thereby opening a novel diagnostic for pre-flare conditions—though the study's reliance on a single event and marginal signal depths call for broader surveys and targeted MHD simulations to firmly establish causality and generality [13].

In this study, we present three flare events displaying characteristic VLPs prior to flare initiation. Section 2 outlines the classification of flares and their associated phases. Section 3 summarizes the approaches used to predict solar flare occurrences. In Section 4, we focus on the generation mechanisms of pre-flare VLPs. Section 5 is dedicated to our observational data and corresponding calculations. Finally, conclusions are drawn and discussed in Section 6.

2 Flare Classification and its Developmental Phases

Solar flares are intense bursts of electromagnetic energy originating from the Sun's atmosphere, spanning wavelengths from radio waves to gamma rays. They are primarily triggered

by the sudden release of magnetic free energy stored in active regions of the solar corona, often linked to electric currents. This release can also lead to particle acceleration and coronal mass ejections (CMEs). Flares are classified based on soft X-ray (SXR) flux measurements in the 1–8 angstrom range by GOES satellites. The classification includes five categories: A, B, C, M, and X In this framework, Class X flares are the most intense with peak flux $> 10^{-4}$, whereas Class A flares are the weakest with peak flux $< 10^{-7}$ [1] (see [5], Baker1970, [2], and [25]). Each class differs by a factor of ten in energy, and a numeric suffix (e.g., X1, X2) provides finer resolution. Flares below Class C typically have negligible Earth impacts, while M and X-class flares can disrupt radio signals and affect satellites. The strongest flare recorded between 1975 and 2004 occurred on November 4, 2003, reaching at least an X28 level, possibly as high as X45, overwhelming GOES detectors [21]. Historically, flares were also classified by their H spectral features based on intensity and radiation output. The full development of a flare includes several phases:

1. *Pre-Flare Phase*: Lasting 10 minutes to an hour before the flare, this phase involves magnetic field reorganization, often due to new magnetic flux. X-ray intensity gradually rises, gas within loops is preheated, and increased filament activity is observed [1,17].

2. *Impulsive Phase*: A brief, energetic stage (100–1000 seconds) marked by hard X-ray, gamma ray, and microwave emissions. Particle acceleration is prominent, especially near magnetic loop footpoints. Some flares, called Masuda flares, show emissions from loop tops [1,14].

3. *Rise (or Flash) Phase*: This stage lasts a few minutes to an hour, with a sharp increase in soft X-ray and H emissions. Particle acceleration and coronal heating continue, raising plasma temperatures to tens of millions of Kelvin.

4. *Quiet (Gradual) Phase*: The flare's energy output declines gradually over hours or even a day. Flares vary in structure—impulsive flares erupt suddenly, while gradual flares evolve more slowly. Emissions include soft X-rays, UV lines, visible light, and radio waves [17].

In impulsive flares, the H response closely follows hard X-ray bursts, indicating electron-beam-driven energy transport. Flare ribbons expand and slow down as the flare evolves, forming post-flare loops that can remain visible for days.

Chromospheric evaporation occurs when energetic particles heat the chromosphere to coronal temperatures. Hot plasma fills the loops, and as the flare declines, this plasma drains back. Total flare energy can range from 10^{19} J in small events to 610^{25} J in the largest, often matching CME kinetic energy. Radiation during the flare mainly occurs in the rise phase, though impulsive emissions contribute significantly at high energies. Fast particles also convert kinetic energy into radiation. While radiation explains part of the energy budget, most energy is stored magnetically in the corona's active regions. Observations confirm that visible and near-UV wavelengths dominate radiative output, but magnetic fields are the ultimate energy source [17].

[1] A-class: $10^{-8} \leq F < 10^{-7}$, B-class: $10^{-7} \leq F < 10^{-6}$, C-class: $10^{-6} \leq F < 10^{-5}$, M-class: $10^{-5} \leq F < 10^{-4}$, X-class: $F \geq 10^{-4}$.

3 Developed Methods for Forecasting Solar Flare Occurrence

Solar flares can significantly impact Earth's space environment, particularly the ionosphere, and trigger geomagnetic storms that weaken Earth's magnetic shield. These storms may cause disruptions in communication, GPS accuracy, and power grids. To prevent such hazards, scientists have developed several forecasting methods. These methods differ in their datasets, time windows, and evaluation metrics. for example four main approaches are emphasized:

- **Bayesian Event Statistics:**
  This method uses historical flare data to predict future events. It assumes that active regions tend to repeat past behavior. The model updates probabilities with each new flare, showing strong predictive power using soft X-ray data [3,17].

- **Automated Solar Activity Prediction (ASAP):**
  This technique integrates machine-learning with image-processing to detect sunspots and active regions. It works in two modes:

  - Image mode: Processes SOHO/MDI images to identify and classify sunspots.
  - Machine-learning mode: Trains neural networks using past flare data to forecast flare class and likelihood.

  The system uses two neural networks: the first predicts whether a flare will occur, and the second classifies the flare as C, M, or X class. It relies on features such as the McIntosh classification and sunspot area [4].

- **Magnetic Field Analysis Using SDO/HMI:**
  High-resolution vector magnetograms from SDO show that flare onset is linked to magnetic field changes, especially near the polarity inversion line (PIL). Studies revealed that most X-class flares involve significant increases in horizontal magnetic field strength near the PIL, which can act as early indicators of flare activity [33].

- **Pre-Flare Fluctuation Monitoring:**
  This method studies long-period soft X-ray fluctuations in the pre-flare phase, usually occurring 10–60 minutes before a flare. Observed quasi-periodic pulsations (QPPs) and very long-period pulsations (VLPs) may signal flare onset. These oscillations are likely linked to magnetohydrodynamic waves or magnetic reconnection events [16].
  Multiple studies have documented VLPs before major flares, with periods between 8–30 minutes, offering valuable precursors for prediction models. Together, these methods—ranging from statistical to machine-learning and magnetic field analysis—represent complementary strategies for improving solar flare forecasts and protecting Earth's technological systems [22].

4 Pre-Flare VLPs and their Generation Mechanism

Pre-flare very long-period pulsations (VLPs) are oscillations observed before solar flares, with unclear origins. While quasi-periodic pulsations (QPPs) during flares are often explained by magnetohydrodynamic (MHD) waves, applying this model to the pre-flare phase is more complex, as no explosive energy release has yet occurred. One theory proposes that twisted

magnetic loops in active regions behave like LRC circuits, due to electric currents generated by footpoint shearing. These currents store magnetic energy and induce oscillations

$$C = \frac{8\pi\rho s^2}{\mu_0^2 l I^2}; L = \frac{\mu_0 l}{\pi}(\ln\frac{8l}{\sqrt{\mu s}} - \frac{7}{4}), \tag{1}$$

where $\rho = n_e m_e + n_i m_i \approx n m_i$ (kg.m^{-3}) is the plasma density, n is the plasma number density, S the cross-section (m^2), l the loop length, and I the electric current. The period increases with S and decreases with I. For typical pre-flare conditions (e.g., $n = 10^{16} m^{-3}$, $l = 5 \times 10^7 m$, a 50-minute, the inferred loop current is on the order of $10^1 0$ A —consistent with observations.

This *LRC* circuit exhibits an intrinsic oscillation with a period of [22]

$$P = 2\pi\sqrt{LC} \approx 2.75 \times 10^4 \frac{s\sqrt{\rho}}{l}. \tag{2}$$

These oscillations can modulate soft and hard X-ray emissions. Pre-flare VLPs are more common in intense flares with short rise times, reflecting faster energy release and simpler loop structure [22,28].

4.1 Assessing the Criteria for Identifying Pre-Flare VLPs

To qualify as a pre-flare VLP, an observed pulse train must meet all of the following:

- Occur within two hours before flare onset.
- Persist for more than 30 min (D > 30 min) and comprise at least four pulses.
- Exhibit a peak amplitude in each pulse exceeding 2σ, where σ is the standard deviation of the background temperature prior to the pulse train.
- Have successive pulse intervals (periods P) satisfying $P_{min} > 1$ and $P_{max} < 2P_{min}$.

A flare is classified as accompanied by pre-flare VLPs if such pulsations appear in the two hours before its onset; if not, it is considered without pre-flare VLPs. Analyses should focus on isolated flares—defined as having no flares of equal or greater magnitude in the preceding two hours and no corrupted data—to avoid external disturbances [22].

5 Data and Observations

For this study, we selected isolated flares spanning a full 24-year solar cycle, as observed in the GOES satellite's soft X-ray channels (1–8 Åand 0.5–4 Å) with a 2 s cadence (`https://satdat.ngdc.noaa.gov/sem/goes/data/full/`). Each GOES platform carries two X-ray sensors measuring 0.5–4 Å(short channel) and 1–8 Å(long channel). NOAA's Space Weather Prediction Center has recorded these measurements since 1974, archiving them at the National Center for Environmental Information. The detectors employ electron deflection to isolate X-rays. GOES-8 through GOES-12 (series I–M) and GOES-13 through GOES-15 (series NOP) use ion-cell X-ray detectors plus filters that yield nearly identical spectral bandwidths across both series. Despite distinct electronics, their full dynamic range measurements agree except at very low signal levels. In each sensor, the short channel response is defined by the ion cell, while the long channel is set by the beryllium (Be) filter thickness. GOES-13 through GOES-15 record both channels—A (0.5–4 Å) and B (1–8

Å)—simultaneously at 2.048 s cadence, storing results in CSV and NetCDF formats. From GOES-15 CSV data, we extracted 10 flares for analysis.

We chose flares with short rise times to maximize the likelihood of detecting pre-flare pulses, following Tan et al. (2016) [22]. Table 1 summarizes the probed new flares, each flare's class, start and peak times, heliographic location, and active region. For every event, we analyzed data from two hours before onset to half an hour after its end, ensuring isolation—no flares of equal or greater magnitude occurred in the two hours prior—and excluding corrupted records. Using MATLAB, we plotted the soft X-ray light curves at 1–8 Å(or 0.5–4 Å) for each flare. We then applied a Fast Fourier Transform (FFT) to each pre-flare interval to identify dominant periodicities, presenting periodograms.

We also analyzed the pre-flare phase of the X2.0 flare on 2014/09/26 (Tan et al. fitted the tempreture of this falre using the function $a+bt+ct^2cos(\omega t)$ [22]). Using the same function (fit 1, figure 1) we obtained $R^2 = 0.84$. By introducing an additional free parameter into the model yielding $(a + bt + ct^2cos(\omega t + f))$, in fit 2, the goodness-of-fit improved significantly, resulting in better R^2 of 0.99.

The flux curves in Figure 2 and 3 reveal pre-flare VLPs as sequences of pulses with nearly uniform spacing. In the case of the M1.2 flare on 2017/09/06, the pulse amplitude grows toward flare onset, whereas in the M1.5 flare on 2017/09/04—it diminishes, while in the M8.1 flare on 2017/09/08 we do not observe any verified VLPs. Table 1 presents the specifications of the flares and the observed VLP periods. Figure 4 illustrates flare without valid pre-flare VLPs.

Table 1: Periods, obtained for flares with VLP (first three flares) and without VLP (the last flare).

Row	Flares	Date of Occurrence	Start Time	Peak Time	End Time	Location	Period (min.)
1	M1.5	2017/09/04	15:11	15:30	15:33	S06W13	25.2
2	M1.2	2017/09/06	23:33	23:39	23:34	S08W40	43.0, 20.0
3	M8.1	2017/09/08	07:40	07:49	07:58	S10W57	—

6 Discussion and Conclusion

In this paper, we report three new flares (from 2017), of the M class (M1.5, M1.2, and M8.1), and examined them. We chose these flares from the flares that had a shorter rise time. According to the observations of Tan et al. (2016), in such flares, there is a higher probability for pre-flare pulses [22]. To do this, we downloaded GOES 15 data in csv format. In two of them, we observed regular VLPs before the flare occurrence. The periods we observed for the VLPs of these flares are 25.2 for the M1.5 flare, on 9 Sep. 2017, started at 15:11 UT, and two periods of 20.0 and 43.0 for the M1.2 flare occurred on 6 Sep. 2017, started at 23:33 UT. We observed no verified VLPs for the third flare, class of M8.1, on 8 Sep. 2017, started at 7:40. The number of pulses observed in each pre-flare is between 4 and 6. No regular VLP was observed for the last selected flare. Moreover, we examined the X2.0 flare reported by Tan et. al (2016), and showed that if we add a phase difference to the fit free parameters, we could improve the fit goodness, increasing the R-square from 0.84 to 0.99.

As we know, the pre-flare VLPs can be a precursor to the occurrence of flares and help us to have a better understanding of the mechanism of the flare onset. Their detection and

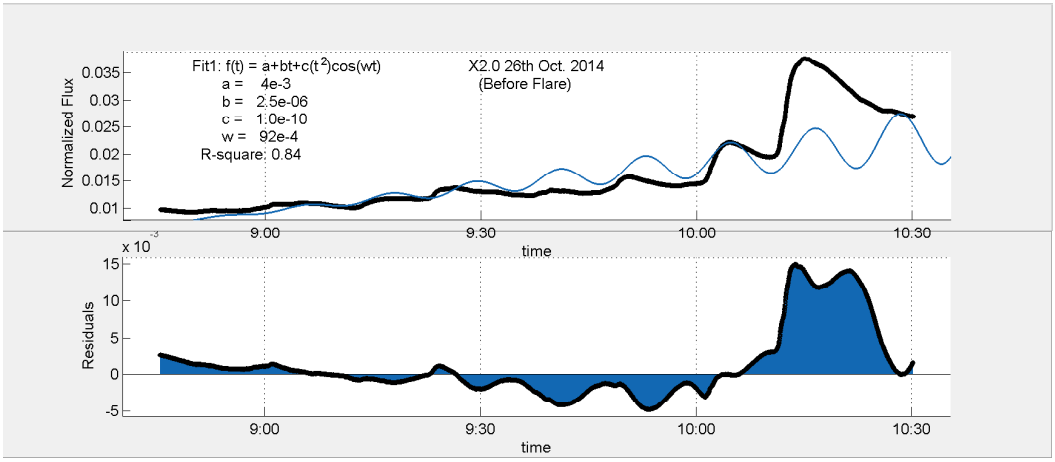

Figure 1: Fit 1: $a + bt + ct^2 cos(\omega t)$. $R^2 = 0.84$

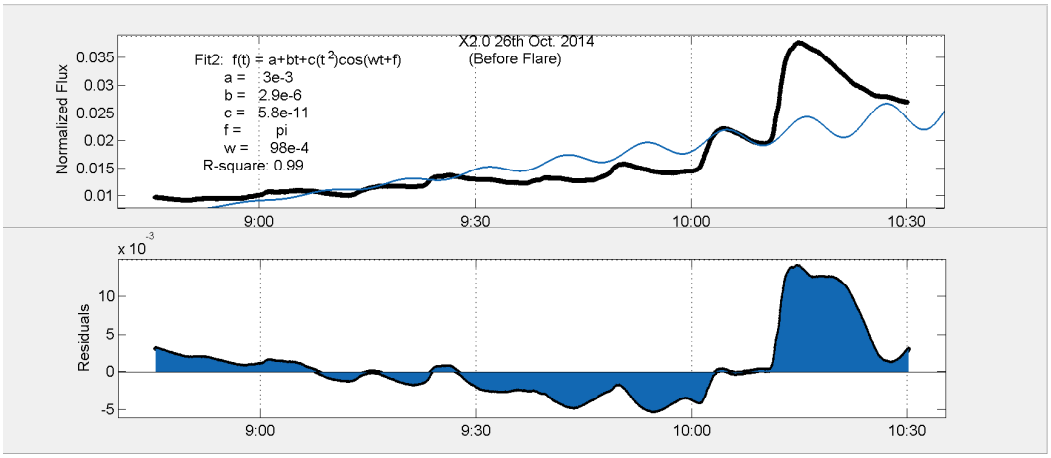

Figure 2: Fit 2: $a + bt + ct^2 cos(\omega t + f)$. $R^2 = 0.99$

Figure 3: Plots of two fits for the pre-flare phase of the Flare X2.0, 26/09/2014.

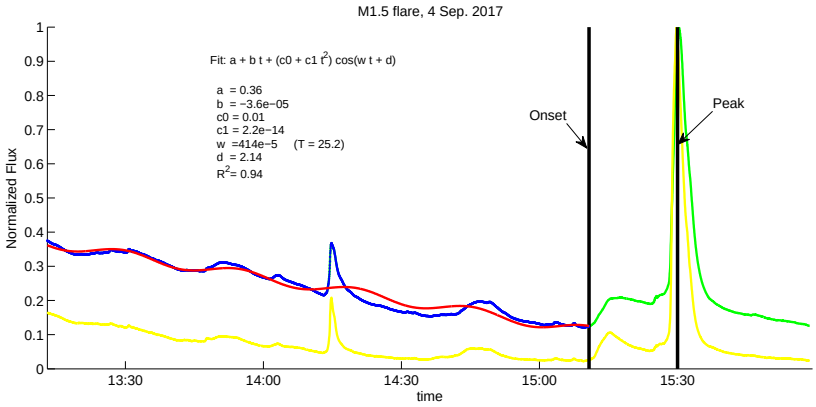

Figure 4: X-ray emission flux of M1.5 flare on 2017/09/04 in which VLP pulsations before the onset of solar flares (pre-flare VLP) have been observed. The green curve is the light curve of the soft X-ray radiation flux at the wavelength of 1-8 Å, and the blue curve shows the pre-flare phase of that and the red one is the fit result. The yellow curve shows the X-ray radiation in the channel of 0.5 - 4Å. Two black vertical lines show the moment of the start and peak of the flare, and the distance between these two lines shows the rising time. These data were obtained from GOES 15 satellite.

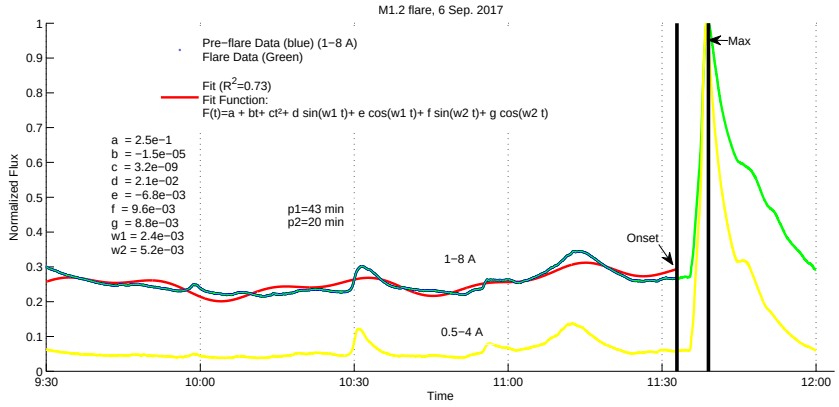

Figure 5: X-ray emission flux of M1.2 flare on 2017/09/06 in which VLP pulsations before the onset of solar flares (pre-flare VLP) have been observed. The green curve is the light curve of the soft X-ray radiation flux at the wavelength of 1-8 Å, and the blue curve shows the pre-flare phase of that and the red one is the fit result. The yellow curve shows the X-ray radiation in the channel of 0.5 - 4Å. Two black vertical lines show the moment of the start and peak of the flare, and the distance between these two lines shows the rising time. These data were obtained from GOES 15 satellite.)

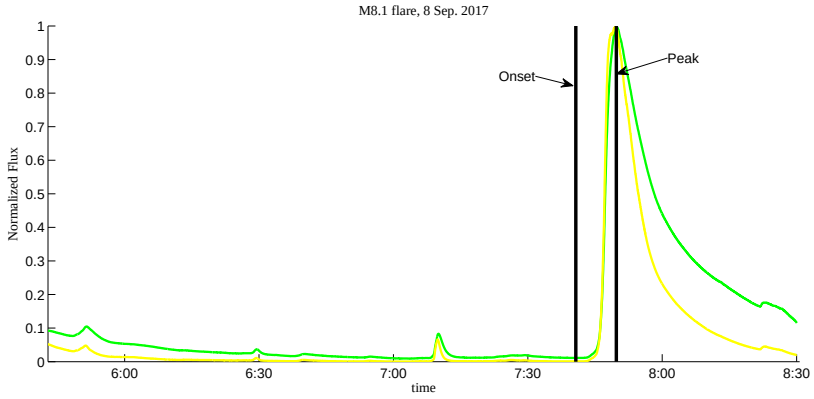

Figure 6: Flare M8.1, 2017/09/08, without pre-flare VLPs.

extraction are also easily possible by GOSE X-ray data, and this allows us to observe them 1-2 hours before flare onset. In all these flares in which we observed pulses or pre-flare VLPs, these VLPs report the occurrence of a flare not too long after. The occurrence of these VLPs can be considered a mechanism for energy release.

Authors' Contributions

All authors have the same contribution.

Data Availability

No data available.

Conflicts of Interest

The authors declare that there is no conflict of interest.

Ethical Considerations

The authors have diligently addressed ethical concerns, such as informed consent, plagiarism, data fabrication, misconduct, falsification, double publication, redundancy, submission, and other related matters.

Funding

This research did not receive any grant from funding agencies in the public, commercial, or nonprofit sectors.

References

[1] Aschwanden, M. 2004, published in association with Prexis Publishing Chichester, UK.

[2] Bai, T. and Sturrock, P. A. 1989, ARA&A, 27, 421.

[3] Baker, D. M., 1970, page 1370. DOI: 10.2514/6.1970-1370.

[4] Colak, T. & Qahwaji, R. 2008, So. Ph., 248(2), 277, DOI:10.1007/s11207-007-9094-3.

[5] Fletcher, L., Dennis, B.R., Hudson, H.S., Krucker, S., Phillips, K., et al., 2011, SSRv, 159, 19.

[6] Harrison, R. A., 1987, Solar soft X-ray pulsations, A&A, 182, 337.

[7] Hayes, L. A., Gallagher, P. T., Dennis, B. R., Ireland, J., Inglis, A. & Morosan, D. E., 2019, ApJ, 875, 33.

[8] Inglis, A. R., Ireland, J., Dennis, B. R., Hayes, L. & Gallagher, P., 2016, ApJ, 833, 284.

[9] Jalalirad, M., Fathalian, N. 2022, JESPHYS, 48(2), 347.

[10] Jalalirad, M., Fathalian, N. 2023, IJAA, 10(2), 201.

[11] Kolotkov, D. Y. Nakariakov, V. M. Kupriyanova, E. G. Ratcliffe, H. Shibasaki, K. 2015 A&A, 574, 53.

[12] Li, D., Li, Y., Lu, L., Zhang, Q., Ning, Z. & Anfinogentov, S., 2020, ApJ, 893, L17.

[13] Li, D., Wang, J., & Huang, Y. 2024, [Preprint]. https://arxiv.org/abs/2408.15706.

[14] Masuda, S., Kosugi, T. Hara, H. & et al. 1994, Nature, 371, 495.

[15] McLaughlin, J. A., Nakariakov, V. M., Dominique, M., Jelínek, P. & Takasao, S., 2018, Space Sci. Rev., 214, 45.

[16] Nakariakov, V. M., Kosak, M. K., Kolotkov, D. Y., Anfinogentov, S. A., Kumar, P. & Moon, Y. J., 2019, ApJ, 874, L1.

[17] Priest, E. First published 2014, Cambridge University Press, NewYork, NY10013-2473, USA.

[18] Pugh, C. E., Broomhall, A.-M. & Nakariakov, V. M., 2019, A&A, 624, A65.

[19] Shen, Y. D., Liu, Y., Su, J. T., Li, H., Zhang, X. F., Tian, Z. J., Zhao, R. J.& Elmhamdi, A., 2013, So.Ph., 288, 585.

[20] Svestka, Z. 1994, So.Ph., 152, 505.

[21] Thomson, N.R., Rodger, C.J. Dowden, R.L. 2004, Geophys. Res. Lett., 31, L06803, DOI:10.1029/2003GL019345.

[22] Tan, B. Yu, Z. Huang, J. Tan, C. & Zhang Y. 2016. ApJ, 833. 206T. https://arxiv.org/abs/1610.09291

[23] Tan, B., Yan, Y., Tan, C. & Liu, Y., 2007, ApJ, 671, 964.

[24] Tan, B. L., Zhang, Y., Tan, C. M., Liu, Y. Y., 2010, APJ, 723, 25.

[25] Tandberg-Hanssen, E., Emslie, A., 1988, The Physics of Solar Flares (Chap.1), Cambridge University Press.

[26] Thurgood, J. Pontin, D. McLaughlin, J. 2017, shin.confE. 88T.

[27] Tian, H., Young, P. R., Reeves, K. K., Wang, O., Antolin, P., Chen, B. & He, J., 2016, ApJ, 823, L16.

[28] Tobias, S. M. & Cattaneo, F., 2013, Nature, 497, 463.

[29] Van Doorsselaere, T. Kupriyanova, E. G. & Yuan, D., 2016, So. Ph., 291, 3143.

[30] Wang, H. Yuan, Y. Shih, F. Y. & Jing, J. 2011, Vol. 273, IAU Symposium, 446.

[31] Wang, T., Ofman, L., Sun, X., Provornikova, E. & Davila, J. M., 2015, ApJ, 811, L13.

[32] Yu, S. & Chen, B. 2019, ApJ, 872, 71Y.

[33] Zekun Lu, Weiguang, C. Gaoxlang, J. Yining, Zh. Mingde, D. & Yang, G. 2019, https://arxiv.org/abs/1803.08310v2